Elia G, Rouainia M, Karofyllakis D, Guzel Y.

Modelling the non-linear site response at the LSST down-hole accelerometer array in Lotung.

***Soil Dynamics and Earthquake Engineering* 2017, 102, 1-14.**

Title:

Modelling the non-linear site response at the LSST down-hole accelerometer array in Lotung

Authors:

Gaetano Elia[1], Mohamed Rouainia[2], Dimitrios Karofyllakis[3] and Yusuf Guzel[4]

[1] Lecturer in Geotechnical Engineering (Ph.D.), School of Civil Engineering & Geosciences, Newcastle University, NE1 7RU - Newcastle Upon Tyne, UK (corresponding author).

E-mail: gaetano.elia@ncl.ac.uk. Phone: +44 (0)191 2087934. Fax: +44 (0)191 2085322

[2] Reader in Computational Geomechanics (Ph.D.), School of Civil Engineering & Geosciences, Newcastle University, NE1 7RU - Newcastle Upon Tyne, UK.

E-mail: mohamed.rouainia@ncl.ac.uk

[3] Ph.D. candidate, School of Civil Engineering & Geosciences, Newcastle University, NE1 7RU - Newcastle Upon Tyne, UK.

E-mail: d.karofyllakis@newcastle.ac.uk

[4] Ph.D. candidate, School of Civil Engineering & Geosciences, Newcastle University, NE1 7RU - Newcastle Upon Tyne, UK.

E-mail: y.guzel@newcastle.ac.uk

Abstract

Down-hole array observations are extremely useful to investigate site amplification effects and to validate numerical modelling techniques for site response. In this paper the ground response of the Lotung experiment site (Taiwan), measured along a down-hole accelerometer array during a weak and a strong motion event, is simulated using different numerical techniques of increasing level of complexity: 1) a simple equivalent-linear visco-elastic procedure, 2) a total stress time-domain scheme using a pressure-dependent hyperbolic model and 3) a fully-coupled approach implementing an advanced elasto-plastic soil model. The numerical models are calibrated against resonant column data and in-situ cross-hole measurements. The two horizontal components of the input motion are applied separately at bedrock level. The results of the simple and advanced numerical simulations are compared with the down-hole motions recorded in-situ during the investigated seismic events in terms of acceleration time histories and response spectra. The comparison between in-situ measurements and predicted results highlights the well-known limitations of the frequency-domain technique. It also shows some improved predictive capabilities of the total stress time-domain scheme and demonstrates the excellent performance of the fully-coupled advanced non-linear approach.

Keywords:

Seismic ground response analysis; Lotung experiment site; Equivalent-linear visco-elastic approach; Elasto-plastic constitutive models; Non-linear time-domain analysis

1. Introduction

Experience from historical and recent strong earthquakes has demonstrated the significance of local soil conditions on the seismic ground response. The changes in amplitude, frequency content and duration of the seismic motion during its propagation in soil deposits, commonly referred to as "site effects", have a crucial impact on the response of buildings and infrastructures during earthquakes [e.g. 1]. The analysis of site effects has been the object of many national and international research projects during the past decades. Following the devastating effects of surface geology on shaking damage observed during the 1985 Mexico City earthquake, the Turkey Flat (California, USA) and Ashigara Valley (Japan) strong motion arrays have been established within the 1992 ESG-IASPEI/IAEE project to help determine the state-of-practice in estimating the effects of surface geology on earthquake ground motion [2-5]. In 1993 the European Commission funded the initial development of the EuroSeisTest[1] programme in Northern Greece for the analysis of structural response to ground motion and the effects of surface geology, non-linear soil response and soil-structure interaction on ground motion. Since then, the monitored site has provided researchers with high-quality multidisciplinary data for conducting theoretical studies on ground response analysis. Wave propagation problems in natural soil deposits have also been studied during the ReLUIS[2] projects (ReLUIS-DPC 2005-2008 and 2010-2013) funded by the University Network of Seismic Engineering Laboratories in Italy. More recently, an international benchmark on the uncertainty assessment associated to non-linear simulation of one-dimensional (1D) site effects has been set up in 2013 within the project PRENOLIN [6] as part of two larger projects: SINAPS@[3], funded by the French National Research Agency (ANR), and SIGMA[4], funded by a consortium of nuclear facility operators (EDF, CEA, AREVA, ENEL). These are only few examples that confirm the ongoing

[1] http://euroseisdb.civil.auth.gr/
[2] http://www.reluis.it/
[3] http://www.institut-seism.fr/en/projects/sinaps/
[4] http://projet-sigma.com/index.html

interest in site response analysis of the international research community working in the broad field of geotechnical earthquake engineering.

Ground response problems can be studied by geotechnical engineers using different numerical approaches, ranging from simplified frequency-domain analyses based on visco-elasticity [7, 8] to time-domain schemes whereby the solid-fluid interaction can be accounted for by means of a coupled effective stress formulation and sophisticated non-linear constitutive models can be adopted to describe the soil cyclic mechanical behaviour [9-12]. For validation purposes, the performance of these different numerical approaches has been tested over the last decades using real vertical array observations. In this case, the input motion is reasonably well defined, as it is directly recorded on rock. As an example, since the establishment in 1996 of the KiK-net array monitoring system in Japan, different researchers have effectively used the available array data for their numerical site response investigations [e.g. 13-19]. In particular, Aguirre and Irikura [20] simulated the response of the Port Island site in Kobe during the 1995 Hyogo-ken Nanbu earthquake using a finite difference program implementing a hyperbolic non-linear model and comparing the results with the recorded down-hole array data. The acceleration time histories were reasonably predicted at depth but the dynamic response of the site was overestimated at surface, as liquefaction occurring in the top 16 m could not be captured by the adopted constitutive model. Another interesting numerical validation is presented by Huang *et al*. [21], who simulated the site response of the Dahan down-hole array in Taiwan subjected to a foreshock weak motion and the main shock of the 1999 Chi-Chi earthquake using the Haskell matrix method based on linear elastic shear wave propagation equations in multi-layered solid media. The horizontal accelerations were accurately predicted when the weak motion was considered. However, the seismic response during the main shock was not satisfactorily predicted due to the inability of the adopted linear elastic model to reproduce non-linear soil behaviour. Also located in Taiwan, the Lotung Large-Scale Seismic Test (LSST) site has been

extensively studied since its establishment in 1985 by a number of authors [22-33]. In particular, Li *et al*. [22] modelled the multi-directional site response at Lotung by employing a fully-coupled finite element (FE) method with a bounding surface hypoplasticity soil model. Satisfactory predictions were obtained for the response in the horizontal direction, whereas the vertical site response was significantly underestimated by the analysis. Similarly, Borja *et al*. [23] and Borja *et al*. [26] studied the dynamic response at Lotung under the simultaneous application of the three components of the earthquake by employing a 3D FE program and a bounding surface elasto-plastic soil constitutive model. Good agreement was observed for all three directions of loading between predicted acceleration time histories and recorded data. However, the adopted soil constitutive model was formulated in terms of total stress, not accounting for solid-fluid interaction effects. Amorosi *et al*. [29] attempted to predict the horizontal site response at Lotung using a fully-coupled effective stress FE program implementing an advanced kinematic hardening multi-surface model. The numerical predictions were in good agreement with recorded data in terms of frequency content, although a significant underestimation of the peak ground acceleration at surface was observed for both components of the input motion. Very recently, Amorosi *et al*. [33] have adopted a three-dimensional FE non-linear approach and applied the two horizontal components of the seismic motion singularly or simultaneously to investigate the role of the input multi-directionality effects on the site response at Lotung. A good agreement with the free-field measurements has been obtained when a single input motion is considered, whereas the simultaneous application of the two horizontal components has produced a slight overestimation of the peak accelerations and the rise of spurious high frequencies.

Even though extensive research has been conducted in recent years on the analysis of site effects, as demonstrated by the mentioned benchmark projects and validation studies, fundamental questions, such as the importance of multi-directional loading and the predictive capabilities of

effective stress advanced soil constitutive models, still need to be answered.

This paper presents a new validation study of the LSST site in Taiwan using the recordings from the down-hole accelerometer array installed in-situ. In particular, the free-field horizontal site response at Lotung during the weak and strong motion events LSST11 and LSST07 is investigated using the simple equivalent-linear visco-elastic method, a total stress non-linear scheme and a fully-coupled effective stress non-linear approach. In the first part of the paper the geological and geotechnical properties of the LSST site are briefly described. The numerical models adopted for the frequency-domain and the time-domain dynamic simulations are then summarised along with the calibration against in-situ and laboratory data of the soil models used in the analyses. The direct comparison at various depths within the soil deposit between recorded and predicted motions obtained with the different numerical approaches, adopting similar profiles of the small-strain shear modulus consistent with the measured data, is presented in the main part of the paper. Finally, the influence of variation in the initial shear modulus profile of the top layers is explored and conclusions are drawn at the end.

2. The Large-Scale Seismic Test at Lotung

The Large-Scale Seismic Test (LSST) is located in one of the most seismically active region in the North-East of Taiwan. It was originally established in the 1980's to study the dynamic behaviour of two scaled-down nuclear plant containment structures [34]. The site response has been monitored by a number of surface and down-hole accelerometer arrays, together with pore pressure transducers. The down-hole accelerometers have been installed at depths of 0, 6, 11, 17 and 47 m, oriented in N-S, E-W and vertical directions. Figure 1 shows the elevation and plan views of the instrumentation. Of particular interest here is the vertical array named DHB in Figure 1a which has been considered representative of the free-field response at Lotung. The site geology consists of recent alluvium and Pleistocene materials over a Miocene basement. The

upper alluvial layer, 30 to 40 m thick, consists mainly of clayey-silts and silty-clays [35]. The water table is located approximately at a depth of 1 m. The local geological profile (Figure 2a) shows a 17 m thick silty sand layer above a 6 m thick layer of sand with gravel resting on a stratum of silty clay interlayered by an inclusion of sand with gravel between 29 m and 36 m, as indicated by the SPT log profile reported in Figure 2b.

A series of geophysical seismic tests have been performed to measure shear and compression wave velocities at the LSST site. The shear wave velocity obtained from seismic cross-hole and up-hole tests [36] showed a value of about 100 m/s at the surface reaching a value of about 300 m/s at 60 m depth. The corresponding elastic shear modulus (G_0) data are shown in Figure 2c with open dots. A total unit weight of 19.6 kN/m^3 has been adopted as average value for the entire deposit [37]. In all previous studies, the bedrock formation has been assumed to be at a depth of 47 m, corresponding to the location of the accelerometer DHB-47 shown in Figure 1a. Shear modulus and damping ratio curves have been measured through resonant column and cyclic torsion tests on undisturbed specimens [36, 38]. Alternatively, Zeghal *et al*. [39] have proposed to back-calculate the in-situ moduli ratio curves for Lotung soil based directly on its seismic response recorded along the down-hole arrays during 18 earthquakes which occurred between 1985 and 1986. In particular, different sets of G/G_0-γ and D-γ curves have been developed for the depths of 0-6, 6-11 and 11-17 m, producing for each depth a least-square best fit (SF) as well as an upper (UB) and a lower bound (LB) curve indicative of the possible variations in the material dynamic properties (Figure 3). The shear modulus and damping ratio curves of the soil between 17 and 47 m are assumed to be equal to those from 11 to 17 m, as more detailed data relevant to the deeper material were missing. Therefore, three different materials can be identified along the deposit in terms of dynamic properties, although the inclusions of sand with gravel between 17 and 23 m and 29 and 36 m are characterised by higher values of effective friction angles (according to the SPT data reported in Figure 2b). It is noted

that the lack of a proper characterisation of the deeper materials (i.e. below 17 m) in terms of soil dynamic properties at the LSST site can affect the accuracy of the site response simulations and, therefore, its influence on the seismic wave propagation process has been investigated in the last part of the paper.

3. Numerical simulations

The ground response of the Lotung LSST site has been studied during one weak (i.e. LSST11) and one strong motion event (i.e. LSST07) recorded along the array. As summarised in Table 1, the LSST11 event was characterised by a shallow focal depth, a relatively small magnitude and peak ground accelerations (PGA) of 0.07 g and 0.10 g respectively in the E-W and N-S direction. On the contrary, the LSST07 event was characterised by a higher magnitude and maximum accelerations recorded at ground surface equal to 0.16 g and 0.20 g in the E-W and N-S direction, respectively.

Figures 4a and 4b report the response spectra of the accelerations recorded during the LSST11 event at bedrock (DHB-47), 11 m below surface (DHB-11) and at ground surface (FA1-5) along the E-W and N-S direction. The response spectra of the acceleration recorded at the same depths during the LSST07 event are shown in Figures 4c and 4d. It is important to note that the weak motion LSST11, although characterised by smaller accelerations across the entire spectrum, is richer in high frequencies than the strong motion LSST07. Moreover, the analysis of the LSST11 array data shows a very little alteration of the motion between the bedrock and 11 m depth, with a significant amplification of the seismic wave occurring between 11 m and ground surface, especially in the N-S direction. Similarly, the LSST07 array measurements indicate that in the N-S direction a much more pronounced amplification has occurred in the top 11 m with respect to the E-W component.

The numerical site response simulations of the Lotung LSST site have been performed using the

1D equivalent-linear visco-elastic software EERA [40], the 1D non-linear time-domain software DEEPSOIL [41] and the 2D fully-coupled FE code SWANDYNE II [42]. In all the analyses, the two horizontal components of the seismic event have been applied separately as input motions at the bedrock level (i.e. at 47 m). It should be noted that the simultaneous application of the two earthquake components would represent a more realistic scenario, but this still requires a better understanding of soil cyclic behaviour under multi-directional loading, from both the laboratory and constitutive modelling point of view [e.g. 33]. Therefore, the choice of applying separately the horizontal components of the input motion has been preferred. The main features of the adopted numerical models are discussed in this section of the paper, whereas the comparison between results obtained with the different numerical approaches is presented in the following Section 4.

3.1 Equivalent-linear visco-elastic model

The code EERA is based on the assumption of equivalent-linear visco-elastic soil behaviour. The approach makes use of the exact solution of wave propagation in horizontally layered visco-elastic materials subjected to vertically propagating transient motions [e.g. 43]. The solution is attempted in the frequency-domain. The non-linear variation of soil shear modulus, G, and damping, D, with shear strain is accounted for through a sequence of linear frequency-domain analyses with iterative update of stiffness and damping parameters. For a given soil layer, G and D are assumed to be constant with time during the shaking. Therefore, an iterative procedure is needed to ensure that the properties used in the linear dynamic analyses are consistent with the level of strain induced by the input motion in each layer.

In the presented EERA analyses, the profile of small-strain stiffness shown in Figure 2c has been discretised using constant stiffness sub-strata of 1 m thickness. The statistical fit (SF) curves reported in Figure 3 have been adopted in the visco-elastic simulations for the top layers (i.e.

between 0 and 17 m). From 17 to 47 m the same curves as those relevant to the depth between 11 and 17 m have been considered. EERA simulations have been performed also using the upper bound (UB) and lower bound (LB) curves shown in Figure 3, but the best results have been obtained adopting the SF curves, as discussed later.

3.2 Non-linear time-domain models

To overcome some of the well-known limitations of the equivalent-linear visco-elastic approach, non-linear schemes able to solve the wave propagation problem by direct numerical integration in the time-domain can be employed. The LSST site response has been, therefore, studied with the 1D program DEEPSOIL, which allows to perform time-domain total stress analyses using the MRDF pressure-dependent hyperbolic model [after 44] with extended unloading-reloading Masing rules [after 45]. The non-linear constitutive model allows to capture the influence of confining pressure on shear modulus degradation. In addition, it implements the hysteretic damping reduction factor (MRDF) proposed by Phillips and Hashash [46] to match measured modulus reduction and damping curves simultaneously over a wide range of shear strains. The same profile of small-strain stiffness used in the EERA simulations has been adopted in the DEEPSOIL analyses (Figure 2c). The G/G_0-γ and D-γ curves predicted by the non-linear model for the depths of 0-6, 6-11 and 11-17 m are presented in Figure 3 and the relevant material parameters are reported in Table 2. For more details on the MRDF pressure-dependent hyperbolic model, the reader is referred to [46]. 1% viscous damping has been introduced in the time-domain simulations performed with DEEPSOIL by means of a standard Rayleigh formulation [e.g. 47], using two modes to obtain a frequency dependent dissipation at small strains. In particular, the best simulation results for both horizontal components of the LSST11 event have been obtained using the frequencies of 1.14 Hz and 5.7 Hz. For the E-W component of the LSST07 event, frequencies equal to 0.84 Hz and 2.65 Hz have been selected, whereas the

values of 0.95 Hz and 4.2 Hz have been used for the N-S component, according to the procedure proposed by Amorosi *et al*. [12].

The ground response analysis of the Lotung experiment site has been also undertaken using the two-dimensional fully-coupled finite element code SWANDYNE II. The code performs linear and non-linear dynamic analyses, using the Generalised Newmark method [48] for time integration. In particular, the values of the Newmark parameters selected in all the FE analyses illustrated in this note are $\beta_1 = 0.600$ and $\beta_2 = 0.605$ for the solid phase and $\beta_1^* = 0.600$ for the fluid phase. These values ensure that the algorithm is unconditionally stable, while being dissipative mainly for the high frequency modes [9]. A 5 m wide, 47 m high FE mesh composed by 235 isoparametric quadrilateral finite elements with 8 solid nodes and 4 fluid nodes has been used in the dynamic simulations. The base of the mesh has been assumed to be rigid, while equal displacements have been imposed to the nodes along the vertical sides (i.e. tied-nodes lateral boundary conditions). Base and lateral hydraulic boundaries have been assumed as impervious, while drained conditions have been imposed at the top of the mesh. In order to investigate the effects of soil non-linearity on the wave propagation process, plasticity has been introduced in the SWANDYNE II simulations through the advanced elasto-plastic model (*RMW*) developed by Rouainia and Muir Wood [49]. The *RMW* model allows to reproduce some of the key features of the cyclic behaviour of natural soils such as the decay of the shear stiffness with strain amplitude, the corresponding increase of hysteretic damping and the related accumulation of excess pore water pressure under undrained conditions. The model has been implemented in SWANDYNE II with an explicit stress integration algorithm and a constant strain sub-stepping scheme. *RMW* has been successfully employed to simulate both static [50, 51] and dynamic geotechnical problems [52, 53]. For more details on its formulation and implementation the reader is referred to [49] and [54]. In previous versions of the model a classical hypoelastic formulation was employed for the determination of the bulk and shear moduli, K and G_0. In this

work, the well-known equation proposed by Viggiani and Atkinson [55] for the small-strain shear modulus has been implemented to reproduce the dependency of G_0 on the mean effective stress and overconsolidation ratio:

$$\frac{G_0}{p_r} = A\left(\frac{p'}{p_r}\right)^n OCR^m \quad (1)$$

where A, m and n are dimensionless stiffness parameters, p_r is a reference pressure (equal to 1 kPa), p' is the mean effective stress and OCR is the soil overconsolidation ratio. In the initialisation of the FE model, a higher overconsolidation ratio has been assumed for the upper part of the FE column (from 0 to a depth of 6 m), with an average OCR equal to 4, while a constant OCR of 2 has been imposed for the remaining part of the model. The assumed variation of OCR with depth is deemed to be realistic in accordance with the G_0 data shown in Figure 2c, where a non zero elastic shear modulus of about 20 MPa can be observed near the ground surface (corresponding to a measured shear wave velocity of about 100 m/s). Once the FE model has been initialised by applying the gravity load, a range of possible elastic shear modulus profiles, controlled by the values of the dimensionless stiffness parameters A, m and n in Equation (1), has been investigated. In previous works by Elia *et al.* [31] and Karofyllakis *et al.* [32], a set of stiffness parameters A, m and n constant with depth was assumed. With this adopted initial small-strain stiffness profile, the peak acceleration of the LSST07 E-W motion at ground surface was very well predicted, while the PGA in the N-S direction was under-predicted. A more realistic G_0 profile, which achieves a better calibration of the cross-hole data, has been assumed in this paper (see Figure 2c). The calibration of the remaining *RMW* parameters has been performed through single element simulations of undrained cyclic simple shear (CSS) tests, by imposing different shear strain amplitudes and assessing the predicted

secant shear modulus and the damping ratio for each strain value after a number of cycles (equal to 500) sufficient to reach a steady-state condition. The results of the CSS test simulations are reported in Figure 3 for each depth and compared with the corresponding curves presented by Zeghal *et al*. [39]. A good agreement with the experimental data can be observed at intermediate strain levels, although the model tends to overestimate the damping at large strains. A small amount of viscous damping, equal to 3%, has been introduced into the model through a standard Rayleigh formulation [e.g. 47] to reduce the spurious high frequency spikes and to compensate for the *RMW* underestimation of damping within the small-strain range (Figure 3). Table 3 summarises the *RMW* model parameters adopted for the different soil layers. It should be noted that the anisotropic and structure degradation features of the model have not been considered in the calibration process, given the lack of appropriate experimental data.

4. Results and discussion

In this section, the free-field site response at Lotung predicted during the weak and strong motion events LSST11 and LSST07 by the equivalent-linear visco-elastic method (EERA), the total stress non-linear scheme (DEEPSOIL) and the fully-coupled effective stress non-linear approach (SWANDYNE II with *RMW*) is presented and the numerical results are consistently compared with the corresponding down-hole accelerometer data recorded at the LSST site.

4.1 LSST11 event

Figures 5a and 5b report the acceleration time histories predicted by the three numerical approaches at ground surface and 11 m depth, respectively, when the E-W component of the LSST11 event is applied at the bedrock. The results of the numerical simulations for the N-S component of the same input motion are, instead, presented in Figures 5c and 5d. Given the high frequency content of the LSST11 event, only the first 10 and 5 seconds of the acceleration time

histories obtained during the E-W and N-S motions, respectively, are shown in Figure 5. The corresponding down-hole motions recorded in-situ during the earthquake along the DHB array are also reported in Figure 5. For the same LSST11 E-W and N-S events, the response spectra (5% damping) at ground surface and 11 m depth are presented in Figure 6. Overall, the results obtained with the three different schemes are in good agreement with the measured data, although none of the numerical techniques is able to properly predict the propagation of the high frequencies at ground surface in the E-W direction (Figure 6a) and at 11 m depth in the N-S direction (Figure 6d). Moreover, a better prediction of the maximum acceleration at surface and at 11 m depth is obtained with the fully-coupled non-linear approach in the N-S direction.

The profiles of maximum acceleration (a_{max}) and maximum shear strain (γ_{max}) induced by the E-W motion are shown in Figures 7a and 7b, respectively, whereas the same profiles obtained during the N-S simulations are reported in Figures 7c and 7d. The maximum accelerations recorded along the DHB array during the LSST11 events are shown in Figures 7a and 7c for comparison. The results of EERA and DEEPSOIL are very similar for both components of the earthquake and in good agreement with the array data recorded in the E-W direction (Figure 7a). The better SWANDYNE II prediction of the N-S motion previously observed in terms of maximum acceleration at different depths (Figures 5 and 6) is confirmed by the results presented in Figure 7c. In general, the weak LSST11 motions induce small shear strains in the soil column (in the order of 0.01%), not enhancing non-linear effects in the mechanical behaviour of the soil. Therefore, the performance of the simpler numerical approaches is considered to be satisfactory in this case.

4.2 LSST07 event

In contrast with LSST11, the strong motion characteristics of the LSST07 earthquake are expected to induce higher shear strains in the deposit associated with more soil non-linearity,

thus leading to a more demanding test of the predictive capabilities of the numerical techniques selected in this work.

The results of the numerical simulations for the E-W and N-S components of the LSST07 seismic event are shown in Figure 8 in terms of acceleration time histories and are compared with the corresponding down-hole motions recorded along the DHB array. Figure 9 presents the same results and comparison in terms of response spectra. EERA is able to predict well the E-W motion, particularly at the depth of 11 m, both in terms of peak acceleration and zero crossing. The peak acceleration at ground surface in the E-W direction is slightly overestimated (Figure 8a). On the contrary, a poorer prediction is obtained by applying the N-S component at bedrock level: the equivalent-linear analysis under-predicts the peak acceleration both at ground surface and at the depth of 11 m (Figures 8c and 8d). Moreover, a time shift in the acceleration peak between the recorded and predicted motions can be observed at surface (Figure 8c). It is, in fact, evident from Figures 9c and 9d that EERA is not able to correctly capture the frequency content of the N-S component both at 0 and 11 m depth. A similar performance of the equivalent-linear visco-elastic approach has been observed previously by Borja *et al*. [23] and Amorosi *et al*. [29]. With reference to DEEPSOIL, an overall better agreement with the array data is observed both in terms of acceleration time histories and frequency content of the two motions at different depths. Nevertheless, the total stress non-linear approach tends to underestimates the peak values of the accelerations at all depths. This may be due to the choice of the same set of shear modulus and damping ratio curves for the soil between 17 and 47 m, while a more linear behaviour, associated to the increasing confining pressure, could be assigned to the deeper soil layers as suggested by Suwal *et al*. [30]. The results of the SWANDYNE II simulations show a better prediction of the frequency content of both the E-W and N-S motions than DEEPSOIL and less underestimation of the peak accelerations, a part from the one at 11 m depth in the N-S direction (Figure 9d). With respect to the previous works by Elia *et al*. [31] and Karofyllakis *et al*. [32], the assumption

of a more realistic G_0 profile has not affected the already very good prediction of the E-W motion and has slightly improved the results in the N-S direction by reducing the underestimation of the PGA from 31% to 27%. Nevertheless, none of the adopted numerical schemes is able to properly predict the observed considerable amplification of the LSST07 seismic wave occurring in the top layers of the soil deposit in the N-S direction.

The above observations are confirmed by the results plotted in Figure 10 in terms of a_{max} and γ_{max} profiles obtained with the three numerical approaches by applying the two components of the LSST07 earthquake at bedrock. The level of maximum shear strains induced by the E-W component is between 0.1% and 0.15%, while it ranges between 0.05% and 0.1% in the N-S direction. Higher shear strains are obtained with the *RMW* model in the top 5 m of the column. This is corroborated by the stress-strain curves shown in Figure 11 for soil elements at ground surface, 11 m and 47 m depth. The stress-strain response of the *RMW* model is, in fact, softer at ground surface, being then comparable with that obtained through EERA and DEEPSOIL at deeper depths. Given the level of shear strain induced by the strong intensity earthquake (i.e. max 0.15%), the hysteretic damping provided by both the hysteretic model in DEEPSOIL and the *RMW* model in SWANDYNE II is well within the limits proposed by Zeghal *et al.* [39] reported in Figure 3. Therefore, the under-prediction of the PGAs, especially in the N-S direction, cannot be attributed to over-damping effects.

One of the main advantages of using a fully-coupled non-linear approach in geotechnical dynamic analyses is its ability to predict the development of excess pore water pressures (Δu), related to the accumulation of plastic deformations, during the seismic excitation. This is, obviously, not possible with the equivalent-linear visco-elastic and the total stress non-linear schemes. With this respect, the excess pore water pressure distributions predicted at the end of the SWANDYNE II analyses are shown in Figure 12 for both the LSST07 components. The numerical results are compared with a set of data recorded during the LSST16 event [56], which

was the only earthquake during which excess pore water pressures were measured in-situ. This event was characterised by similar values of peak ground acceleration, epicentral distance and magnitude of those relative to the LSST07 earthquake. The comparison shows a reasonable agreement between recorded and predicted excess pore pressures in the first 20 m of the deposit, for which the data are available.

4.3 LSST07 event with a shortened soil column

In the case of the strong intensity LSST07 earthquake, the analysis of the numerical predictions presented above suggests that the N-S component reaches the depth of 11 m already significantly damped from the deeper soil layers (Figure 9d), for which a proper geotechnical characterization in terms of shear modulus and damping curves is not available. The predicted motion at 11 m obtained in the E-W direction is, instead, in good agreement with the measured in-situ data (Figure 9b). Therefore, to reduce the uncertainty related to the dynamic properties of the bottom layers, further simulations have been undertaken using the fully-coupled non-linear approach and applying the LSST07 motion recorded at 17 m depth (DHB-17 in Figure 1) as the input action at the base of a 17 m FE column. Firstly, a G_0 profile similar to that adopted in the 47 m column fully-coupled FE analyses has been used on the shortened column. This profile is shown in Figure 13 with a solid line (named "RMW") and it matches the average cross-hole data. Figure 14 shows the acceleration time histories obtained with SWANDYNE II. Excellent agreement with the down-hole data can be observed at all depths (i.e. 11 m, 6 m and 0 m) in the E-W direction, while the acceleration peaks are substantially underestimated in the N-S direction. This result is consistent with the observations made on the 47 m column, indicating that the overall propagation is not significantly influenced by the bottom layers of the soil deposit (i.e. below 17 m).

The small-strain shear modulus data obtained from the cross-hole tests at Lotung in the top 17 m

shows a natural variability with a standard deviation of approximately 10 MPa [57]. Therefore, a reduced G_0 profile, still within the limits indicated by the in-situ measurements, has been used in the final set of simulations using the shortened column. The adopted profile is shown in Figure 13 with a dashed line (named "RMW_mod") and represents a lower bound of the experimental data set. The corresponding SWANDYNE II results are reported in Figure 15 for the two earthquake components. Very good agreement with the down-hole data can be observed at 11 m depth in both directions (Figures 15c and 15f) and at 6 m depth in the E-W direction (Figure 15b). The maximum acceleration at ground surface in the N-S direction is almost identical to the measured one (Figure 15d), although the PGA of the E-W component is now overestimated (Figure 15a). The analysis of the 17 m column results confirms the idea that, even adopting the most advanced numerical approach, it is quite difficult to perfectly estimate the peak accelerations at ground surface of both the LSST07 input motions: when the PGA of the E-W component is well captured, the PGA in the N-S direction is under-predicted and, vice versa, when the N-S component is well predicted, the PGA of the E-W motion is overestimated.

5. Conclusion

The ground response analysis of the Large-Scale Seismic Test site in Lotung has been studied in this work using the simple equivalent-linear visco-elastic method (EERA), a total stress non-linear FE technique (DEEPSOIL) and a fully-coupled non-linear FE approach (SWANDYNE II). The incorporation of plasticity, through a hyperbolic model in DEEPSOIL and the advanced *RMW* model in SWANDYNE II, has allowed investigation of the effects of soil non-linearity on the propagation of a weak and a strong motion. The comparison with recorded array data has enabled the assessment of the performance of three numerical schemes and the following conclusions can be drawn:

i) While a weak motion is reasonably predicted by all numerical methods, the equivalent-

linear visco-elastic method cannot capture the frequency content and peak acceleration of the strong intensity event, especially at ground surface. On the contrary, the predictions obtained with the fully-coupled effective stress approach implementing the kinematic hardening elasto-plastic *RMW* model are particularly successful.

ii) The performance of DEEPSOIL sits somehow between a simpler visco-elastic approach and more advanced fully-coupled schemes. The significant underestimation of the peak values of the accelerations during the strong motion event can be possibly attributed to the choice of stiffness and damping curves for the deeper soil layers, as suggested by Suwal *et al*. [30].

iii) The underestimation of the peak accelerations recorded at ground surface during the strong intensity event cannot be attributed to over-damping effects, as the hysteretic damping provided by the hyperbolic and *RMW* models is well within the limits of the experimental data for the shear strain level induced by the earthquake.

iv) The influence of the poor geotechnical information regarding the dynamic properties of the deeper soil layers at Lotung has been analysed by reducing the depth of the investigated soil column to the top 17 m, showing a good dynamic characterisation. The results obtained with the fully-coupled non-linear scheme for the LSST07 strong motion event highlight the importance of the G_0 profile adopted in the simulations. Specifically, a shear stiffness profile plotting on the lower boundary of the experimental data produces a better prediction of the PGA in the N-S direction, although the maximum acceleration during the E-W motion may be overestimated.

v) In this paper, the two horizontal components of the input motions have been applied separately at bedrock level. The recent work by Amorosi *et al*. [33] seems to indicate that the simultaneous application of the two components of the earthquake in 3D FE simulations of the LSST site does not lead to a better prediction of the down-hole data,

possibly due to a less dissipative response of the soil model under multi-directional loading conditions. Nevertheless, further laboratory and constitutive modelling investigation is needed to prove this conclusion.

In general, the presented work highlights the usefulness of down-hole array data for the validation of site response analyses. The paper emphasises the importance of proper site characterisation in terms of soil dynamic properties and the limits and benefits of the currently available numerical techniques for seismic ground response simulations. A parametric analysis performed to simulate different decay curves for the deeper soil layers has not led to important deviations in the results. Nevertheless, the sensitivity of advanced site response models to statistical variations in soil properties represents an area of future research.

Acknowledgements

The Authors would like to thank Stavroula Kontoe from Imperial College London for providing the LSST array data and the two anonymous reviewers for their valuable comments and suggestions.

References

[1] Daniell JE, Vervaeck A. Damaging Earthquakes Database 2012 – The Year in Review. CEDIM Research Report 2013-01, Center for Disaster Management and Risk Reduction Technology, Potsdam, Germany; 2013.

[2] Tucker BE, Real CR. Turkey Flat, USA Site Effects Test Area – Report 1: Needs, Goals, and Objectives. California Division of Mines and Geology, TR 86-1; 1986.

[3] Tucker BE, Real CR. The design and operation of a test site near Parkfield, California to compare and test methods of estimating the effect of surface geology on seismic motion. Proc. Workshop on Earthquake Ground-Motion Estimation in Eastern North America, Electric Power Research Institute EPRI NP 5875; 1988.

[4] Kudo K, Shima E. Installation of strong motion seismographs, plan for geotechnical measurements, at Ashigara valley site effects test area, Japan. Proc. IASPEI/IAEE Joint working group on effects of surface geology on seismic motion second workshop, Japanese working group on effects of surface geology on seismic motion; 1988.

[5] Kwok AOL, Stewart JP, Hashash YMA. Nonlinear ground-response analysis of Turkey Flat shallow stiff-soil site to strong ground motion. Bulletin of the Seismological Society of America 2008;98(1):331-343.

[6] Régnier J, Bonilla LF, Bard PY, Bertrand E, Hollender F, Kawase H, Sicilia D, Arduino P, Amorosi A, Asimaki D, Boldini D, Chen L, Chiaradonna A, DeMartin F, Ebrille M, Elgamal A, Falcone G, Foerster E, Foti S, Garini E, Gazetas G, Gélis C, Ghofrani A, Giannakou A, Gingery JR, Glinsky N, Harmon J, Hashash YMA, Iai S, Jeremić B, Kramer S, Kontoe S, Kristek J, Lanzo G, di Lernia A, Lopez-Caballero F, Marot M, McAllister G, Mercerat ED, Moczo P, Montoya-Noguera S, Musgrove M, Nieto-Ferro A, Pagliaroli A, Pisanò F, Richterova A, Sajana S, Santisi d'Avila MP, Shi J, Silvestri F, Taiebat M, Tropeano G, Verrucci L, Watanabe K. International benchmark on numerical simulations for 1D, nonlinear site response (PRENOLIN): verification phase based on canonical cases. Bulletin of the Seismological Society of America 2016;106(5):2112-2135.

[7] Schnabel PB, Lysmer J, Seed HB. SHAKE: a computer program for earthquake response analysis of horizontally layered sites. Report No EERC72-12, Earthquake Engineering Research Center, University of California, Berkeley; 1972.

[8] Idriss IM, Sun JI. SHAKE91: A computer program for conducting equivalent linear seismic response analyses of horizontally layered soils deposits. Center for Geotechnical Modeling, University of California, Davis; 1992.

[9] Zienkiewicz OC, Chan AHC, Pastor M, Schrefler BA, Shiomi T. Computational Geomechanics (with special reference to earthquake engineering). Wiley & Sons, Chichester; 1999.

[10] Kwok AOL, Stewart JP, Hashash YMA, Matasovic N, Pyke R, Wang Z, Yang Z. Use of exact solutions of wave propagation problems to guide implementation of nonlinear seismic ground response analysis procedures. Journal of Geotechnical and Geoenvironmental Engineering 2007;133(11):1385-1398.

[11] Semblat JF, Pecker A. Waves and Vibrations in Soils: Earthquakes, Traffic, Shocks, Construction works. IUSS Press, Pavia, Italy; 2009.

[12] Amorosi A, Boldini D, Elia G. Parametric study on seismic ground response by finite element modelling. Computers and Geotechnics 2010;37(4):515-528.

[13] Sato K, Kokusho T, Sawada Y, Yajima H. Soil amplification and seismic motion of surface geology included Pleistocene layers in Hyogoken-Nambu earthquake. Proc. 11th World Conference on Earthquake Engineering, Acapulco, Mexico, Paper No. 1180; 1996.

[14] Tai M, Iwasaki YT. Simulation of the 1995 Hyogo-ken-Nanbu earthquake using stochastic Green's function in consideration of site-specific amplifications and phase characteristics. Proc. 11th World Conference on Earthquake Engineering, Acapulco, Mexico, Paper No. 1624; 1996.

[15] Pavlenko OV, Irikura K. Nonlinear behavior of soils revealed from the records of the 2000 Tottori, Japan, earthquake at stations of the digital strong-motion network Kik-Net. Bulletin of the Seismological Society of America 2006;96(6):2131-2145.

[16] Assimaki D, Steidl J. Inverse analysis of weak and strong motion downhole array data from the Mw 7.0 Sanriku-Minami earthquake. Soil Dynamics and Earthquake Engineering 2007;27(1):73-92.

[17] Bonilla LB, Tsuda K, Pulido N, Régnier J, Laurendeau A. Nonlinear site response evidence of K-NET and KiK-net records from the 2011 off the Pacific coast of Tohoku Earthquake. Earth Planets Space 2011;63:785-789.

[18] Kaklamanos J, Bradley BA, Thompson EM, Baise LG. Critical parameters affecting bias and variability in site response analyses using KiK-net downhole array data. Bulletin of the Seismological Society of America 2013;103:1733-1749.

[19] Kaklamanos J, Baise LG, Thompson EM, Dorfmann L. Comparison of 1D linear, equivalent-linear, and nonlinear site response models at six KiK-net validation sites. Soil Dynamics and Earthquake Engineering 2015;69:207-219.

[20] Aguirre J, Irikura K. Nonlinearity, liquefaction, and velocity variation of soft soil layers in Port Island, Kobe, during the Hyogo-ken Nanbu Earthquake. Bulletin of the Seismological Society of America 1997;87:1244-1258.

[21] Huang H-C, Huang S-W, Chiu H-C. Observed evolution of linear and nonlinear effects at the Dahan Downhole Array, Taiwan: Analysis of the September 21, 1999 M7.3 Chi-Chi earthquake sequence. Pure and Applied Geophysics 2005;162:1-20.

[22] Li XS, Shen CK, Wang ZL. Fully coupled inelastic site response analysis for 1986 Lotung earthquake. Journal of Geotechnical and Geoenvironmental Engineering 1998;124(7):560-573.

[23] Borja RI, Chao HY, Montáns FJ, Lin CH. Nonlinear ground response at Lotung LSST site. Journal of Geotechnical and Geoenvironmental Engineering 1999;125(3):187-197.

[24] Borja RI, Chao HY, Montáns FJ, Lin CH. SSI effects on ground motion at Lotung LSST site. Journal of Geotechnical and Geoenvironmental Engineering 1999;125(9):760-770.

[25] Huang H-C, Shieh C-S, Chiu H-C. Linear and nonlinear behaviors of soft soil layers using Lotung downhole array in Taiwan. Terrestrial Atmospheric and Oceanic Sciences 2001;12(3):503-524.

[26] Borja RI, Duvernay BG, Lin CH. Ground response in Lotung: total stress analyses and parametric studies. Journal of Geotechnical and Geoenvironmental Engineering 2002;128(1):54-63.

[27] Lee C-P, Tsai Y-B, Wen K-L. Analysis of nonlinear site response using the LSST downhole accelerometer array data. Soil Dynamics and Earthquake Engineering 2006;26:435-460.

[28] Borja RI, Sun WC. Estimating inelastic sediment deformation from local site response simulations. Acta Geotechnica 2007;2:183-195.

[29] Amorosi A, Elia G, Boldini D, Schiavone F. Seismic ground response analysis: comparison between numerical simulations and observed array data. Proc. 5th Int. Conf. on Earthquake Geotechnical Engineering, Santiago, Chile; 2011.

[30] Suwal S, Pagliaroli A, Lanzo G. Numerical modelling of site response at the LSST downhole array in Lotung. SECED 2015 Conference: Earthquake Risk and Engineering towards a Resilient World, Cambridge, UK; 2015.

[31] Elia G, Karofyllakis D, Rouainia M. Non-linear finite element analysis of site effects at Lotung (Taiwan). SECED 2015 Conference: Earthquake Risk and Engineering towards a Resilient World, Cambridge, UK; 2015.

[32] Karofyllakis D, Elia G, Rouainia M. Seismic ground response at Lotung (Taiwan). COMPDYN 2015, 5th ECCOMAS Thematic Conference on Computational Methods in Structural Dynamics and Earthquake Engineering, Crete Island, Greece; 2015.

[33] Amorosi A, Boldini D, di Lernia A. Seismic ground response at Lotung: Hysteretic elasto-plastic-based 3D analyses. Soil Dynamics and Earthquake Engineering 2016;85, 44-61.

[34] Tang HT, Tang YK, Stepp JC. Lotung large-scale seismic experiment and soil-structure interaction method validation. Nuclear Engineering and Design 1990;123:197-412.

[35] Anderson DG. Geotechnical synthesis for the Lotung large-scale seismic experiment. Tech. Rep. No. 102362, Electric Power Research Institute, Palo Alto, California; 1993.

[36] Anderson DG, Tang YK. Summary of soil characterization program for the Lotung large-scale seismic experiment. Proc. EPRI/NRC/TPC Workshop on Seismic Soil Structure Interaction Analysis Techniques Using Data from Lotung, Taiwan, EPRI NP-6154, Electric Power Research Institute, Palo Alto, California, 1, 4.1-4.20; 1989.

[37] Elgamal AW, Zeghal M, Tang HT, Stepp JC. Lotung downhole array. I: Evaluation of site dynamic properties. Journal of Geotechnical Engineering 1995;121(4):350-362.

[38] EPRI. Guidelines for determining design basis ground motions – Vol. 1: Method and guidelines for estimating earthquake ground motion in Eastern North America. Rep. No. TR-102293, Electric Power Research Institute, Palo Alto, California; 1993.

[39] Zeghal M, Elgamal AW, Tang HT, Stepp JC. Lotung downhole array. II: Evaluation of soil nonlinear properties. Journal of Geotechnical Engineering 1995;121(4):363-378.

[40] Bardet JP, Ichi K, Lin GH. EERA: A computer program for Equivalent-linear Earthquake site Response Analyses of layered soil deposits. Department of Civil Engineering, University of Southern California, Los Angeles, California; 2000.

[41] Hashash YMA, Groholski DR, Phillips CA, Park D, Musgrove M. DEEPSOIL 5.0, User Manual and Tutorial; 2011.

[42] Chan AHC. User Manual for DIANA-SWANDYNE II. School of Engineering, University of Birmingham, UK; 1995.

[43] Roesset JM. Soil amplification of earthquakes. In: Numerical Methods in Geotechnical Engineering, Desai CS and Christian JT eds., McGraw-Hill, New York; 1977.

[44] Matasovic N. Seismic response of composite horizontally-layered soil deposits. Ph.D. Thesis, University of California, Los Angeles; 1993.

[45] Masing G. Eignespannungen und verfestigung beim messing. In: Second International Congress on Applied Mechanics, Zurich, Switzerland, pp. 332-335; 1926.

[46] Phillips CA, Hashash YMA. Damping formulation for nonlinear 1D site response analyses. Soil Dynamics and Earthquake Engineering 2009;29:1143-1158.

[47] Clough RW, Penzien J. Dynamics of Structures. 2nd Edition, McGraw-Hill, New York; 1993.

[48] Katona MG, Zienkiewicz OC. A unified set of single step algorithms Part 3: the Beta-m method, a generalisation of the Newmark scheme. International Journal of Numerical Methods in Engineering 1985;21:1345-1359.

[49] Rouainia M, Muir Wood D. A kinematic hardening constitutive model for natural clays with loss of structure. Géotechnique 2000;50:153-164.

[50] Gonzáles NA, Rouainia M, Arroyo M, Gens A. Analysis of tunnel excavation in London Clay incorporating soil structure. Géotechnique 2012;62(12):1095-1109.

[51] Panayides S, Rouainia M, Muir Wood D. Influence of degradation of structure on the behaviour of a full-scale embankment. Canadian Geotechnical Journal 2012;49:344-356.

[52] Elia G, Rouainia M. Seismic performance of earth embankment using simple and advanced numerical approaches. Journal of Geotechnical and Geoenvironmental Engineering 2013;139(7):1115-1129.

[53] Elia G, Rouainia M. Performance evaluation of a shallow foundation built on structured clays under seismic loading. Bulletin of Earthquake Engineering 2014;12(4):1537-1561.

[54] Zhao J, Sheng D, Rouainia M, Sloan SW. Explicit stress integration of complex soil models. International Journal of Numerical and Analytical Methods in Geomechanics 2005;29(12):1209-1229.

[55] Viggiani GMB, Atkinson JH. Stiffness of fine-grained soil at very small strains. Géotechnique 1995;45(2):249-265.

[56] Tang YK, Tang HT. Lotung Large-Scale Seismic Test strong motion records. Rep. No. NP-7496, Electric Power Research Institute, Palo Alto, California; 1992.

[57] Andrade JE, Borja RI. Quantifying sensitivity of local site response models to statistical variations in soil properties. Acta Geotechnica 2006;1:3-14.

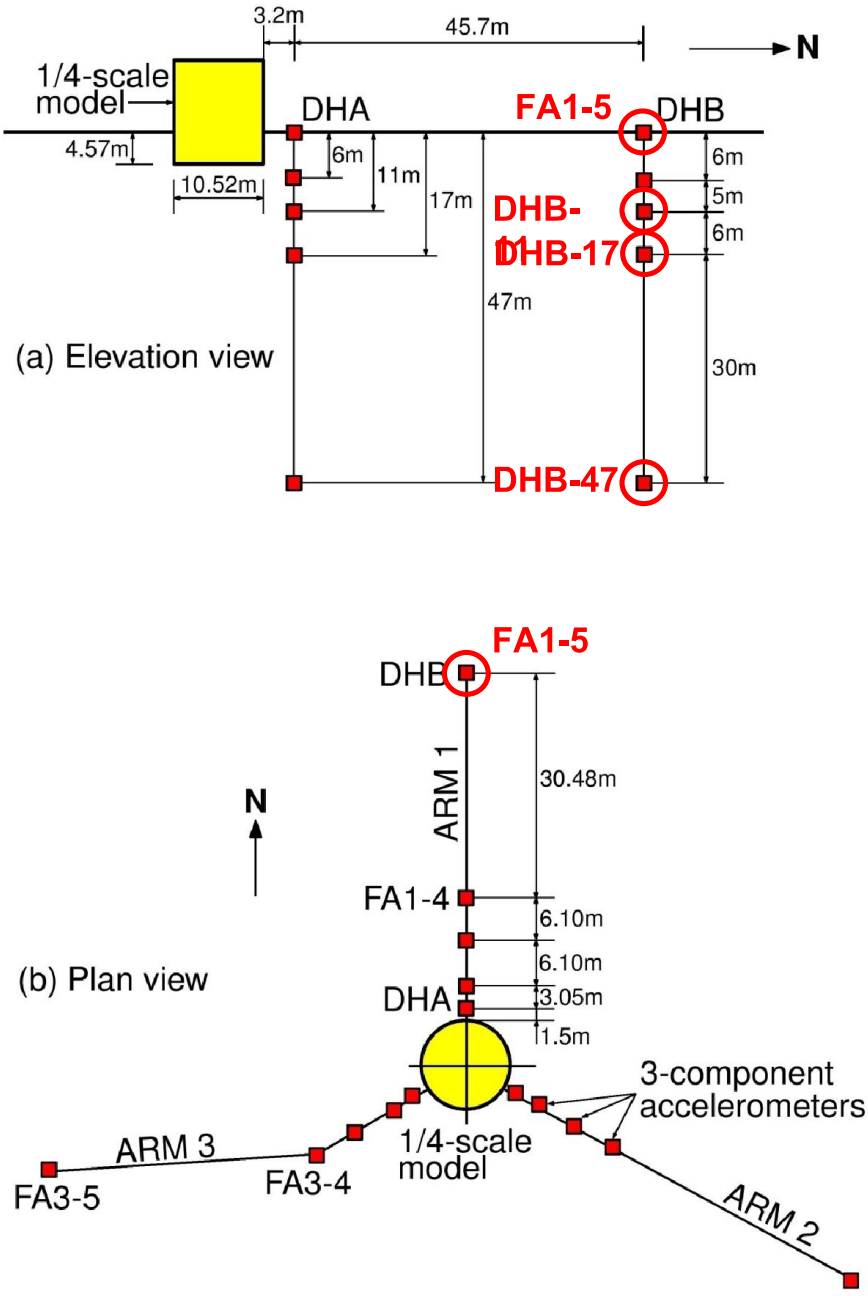

Fig. 1. Location of instrumentation: (a) elevation view; (b) plan view (after Elgamal *et al*. [36]).

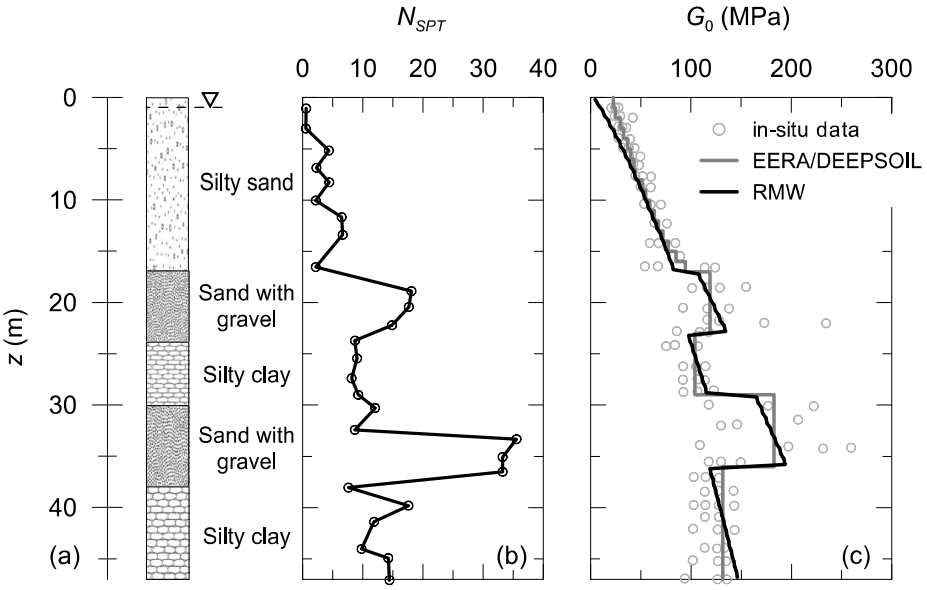

Fig. 2. Local soil profile at LSST site: (a) stratigraphy; (b) SPT log; (c) elastic shear modulus.

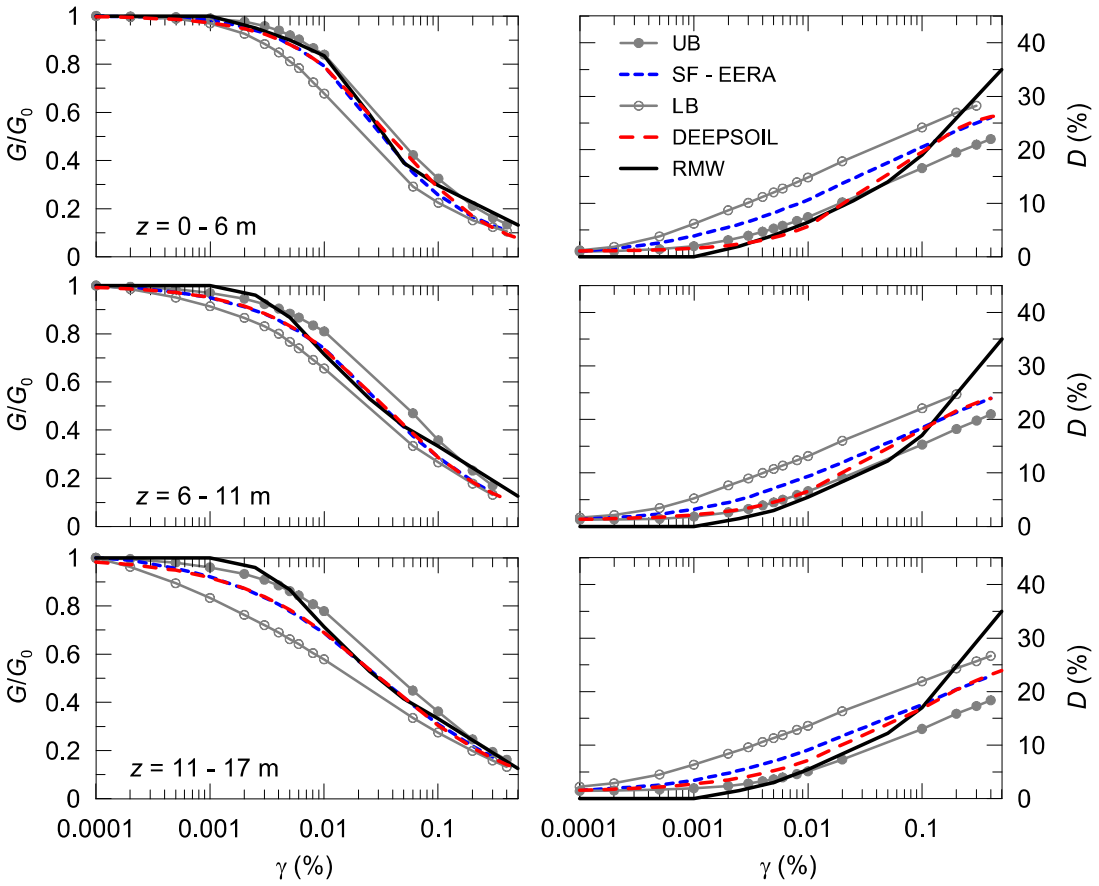

Fig. 3. Shear modulus degradation and damping curves at different depths.

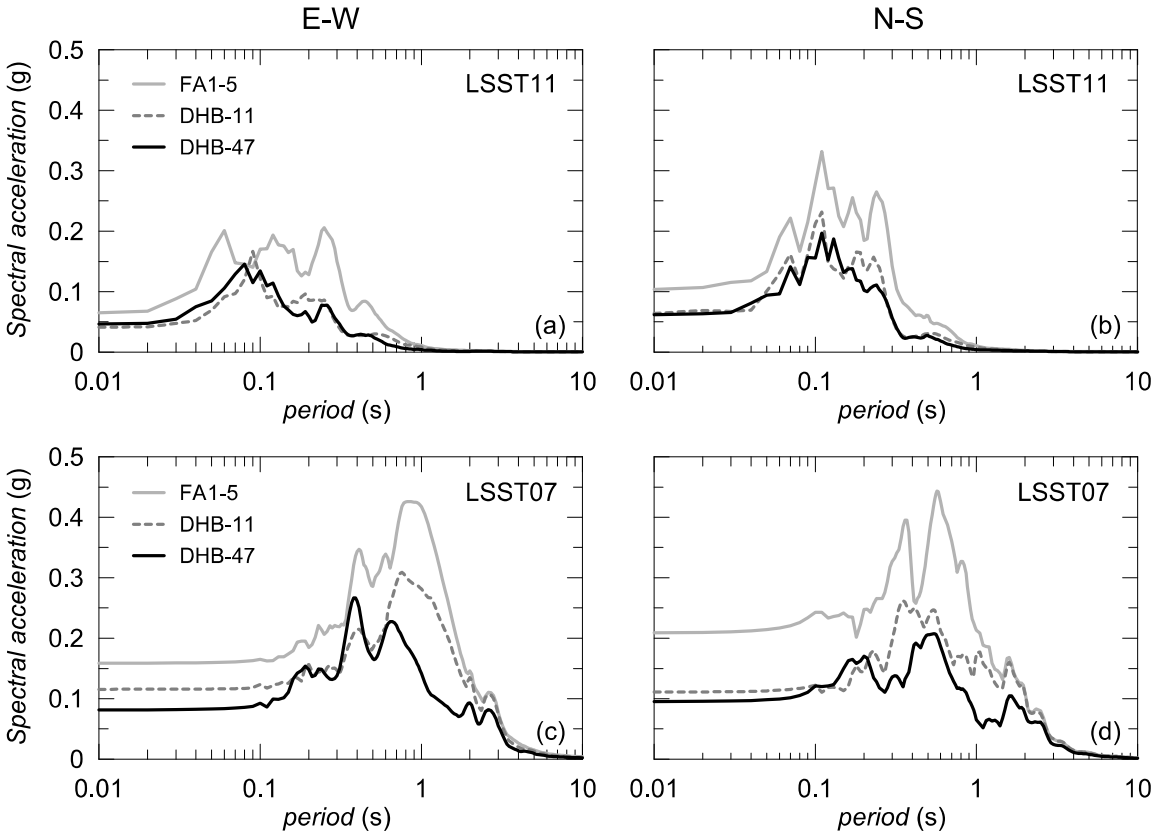

Fig. 4. Response spectra of the accelerations recorded during the LSST11 and LSST07 events.

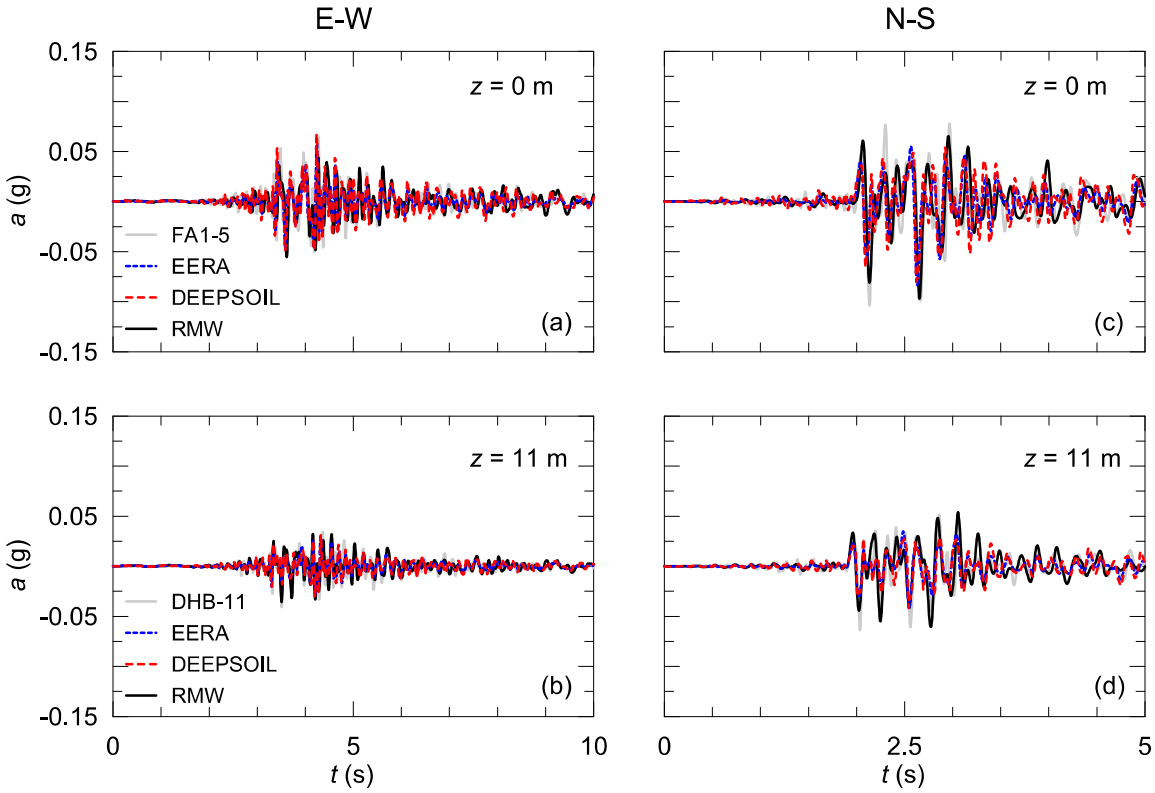

Fig. 5. Comparison between predicted acceleration time histories and LSST11 array data.

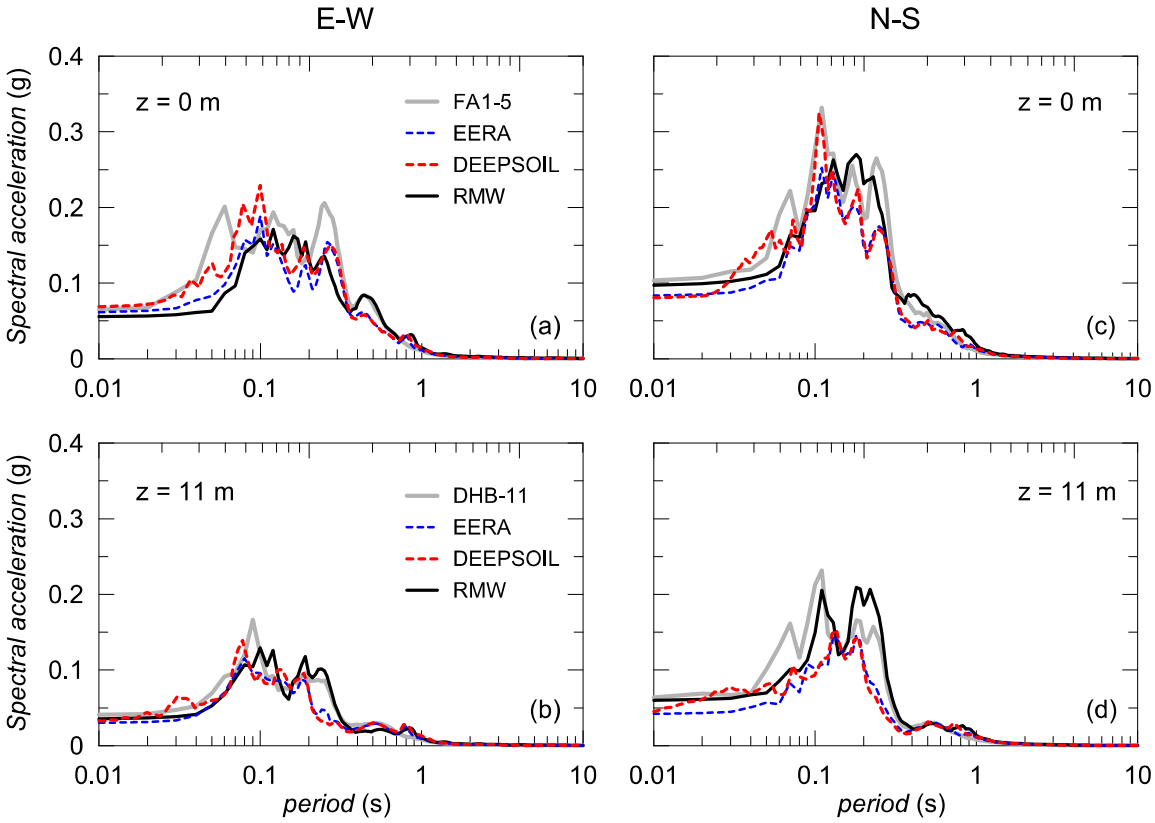

Fig. 6. Comparison between predicted response spectra and LSST11 array data.

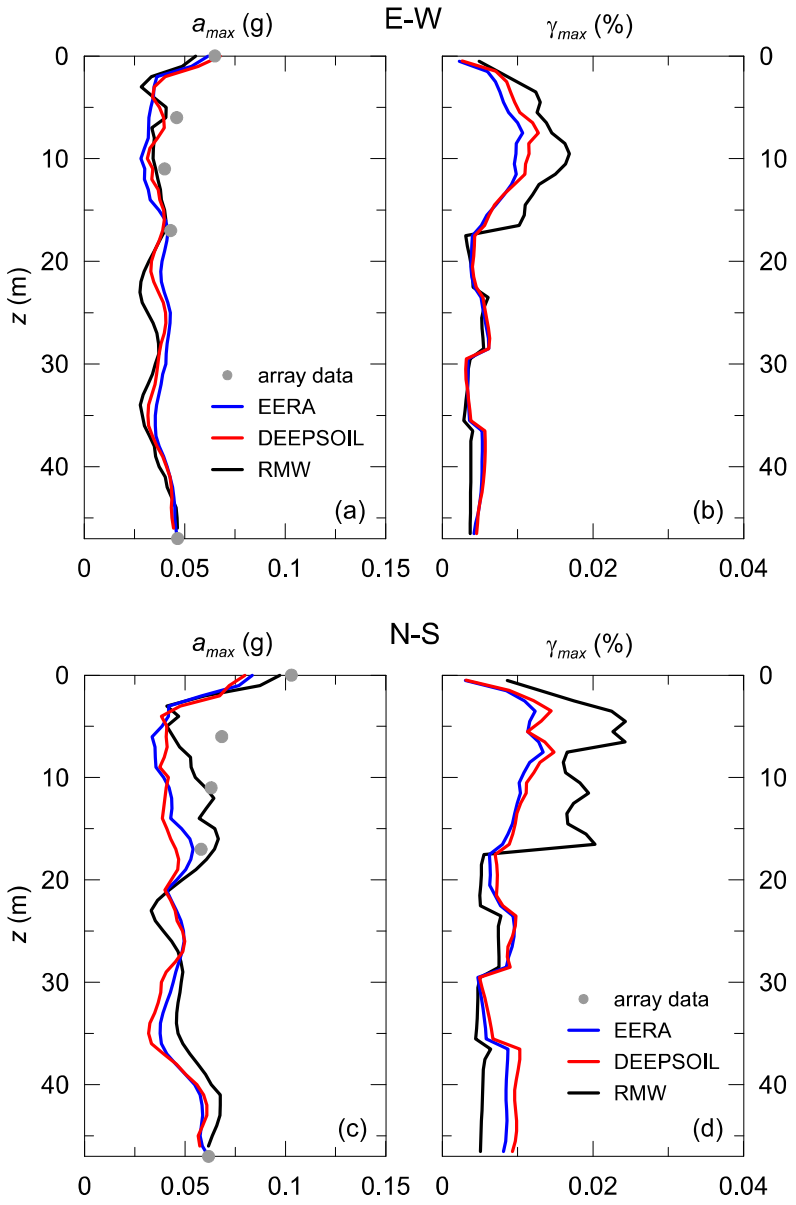

Fig. 7. Comparison between LSST11 array data and numerical predictions in terms of (a, c) maximum acceleration and (b, d) maximum shear strain.

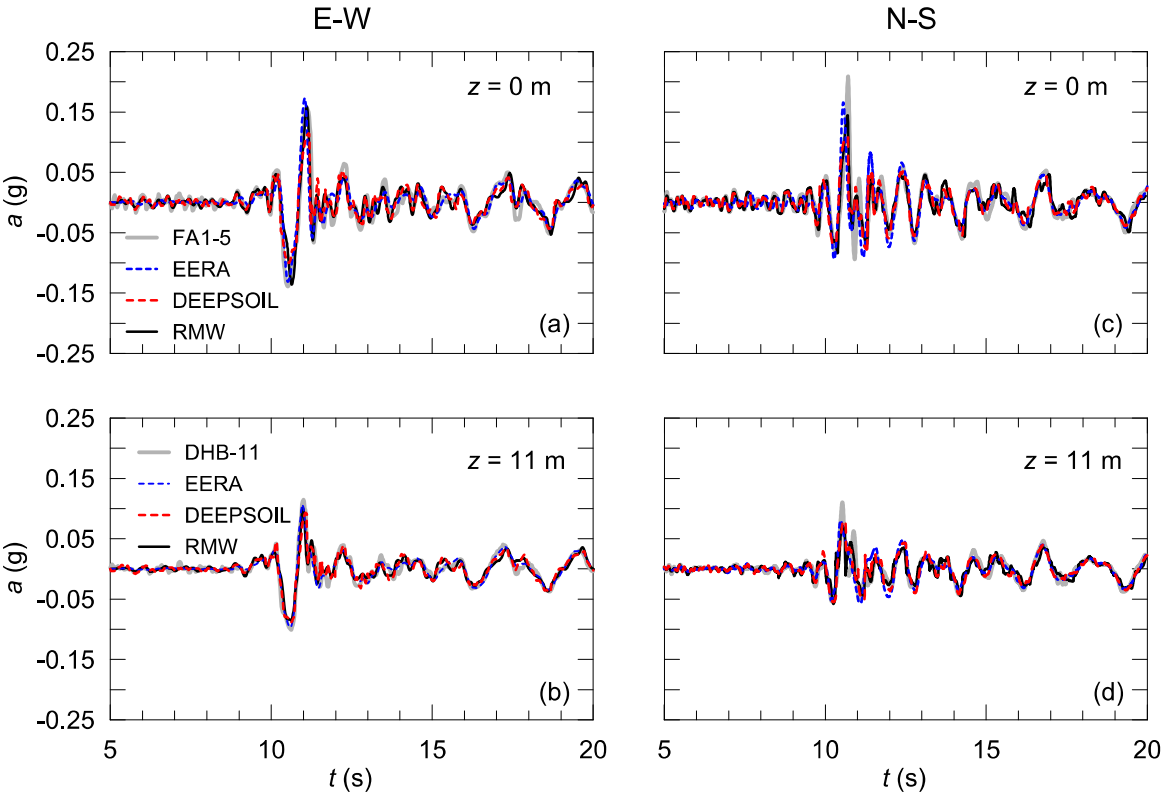

Fig. 8. Comparison between predicted acceleration time histories and LSST07 array data.

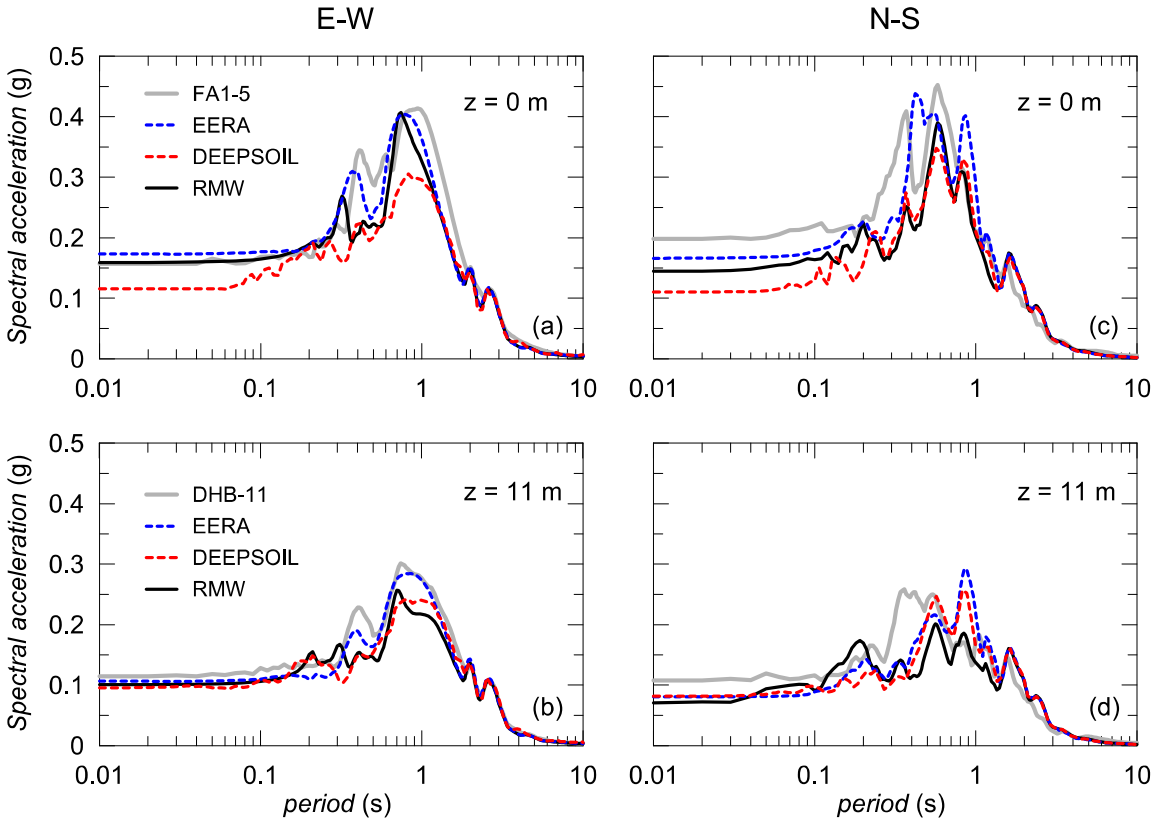

Fig. 9. Comparison between predicted response spectra and LSST07 array data.

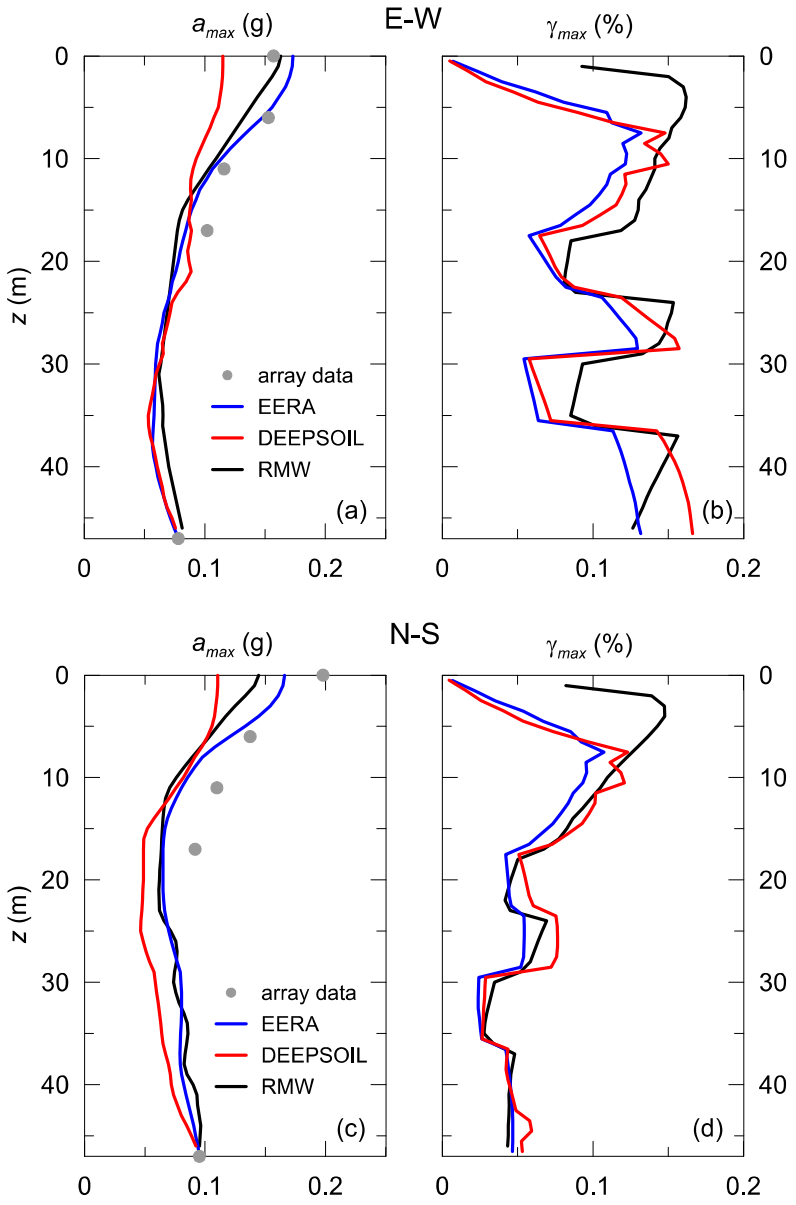

Fig. 10. Comparison between LSST07 array data and numerical predictions in terms of (a, c) maximum acceleration and (b, d) maximum shear strain.

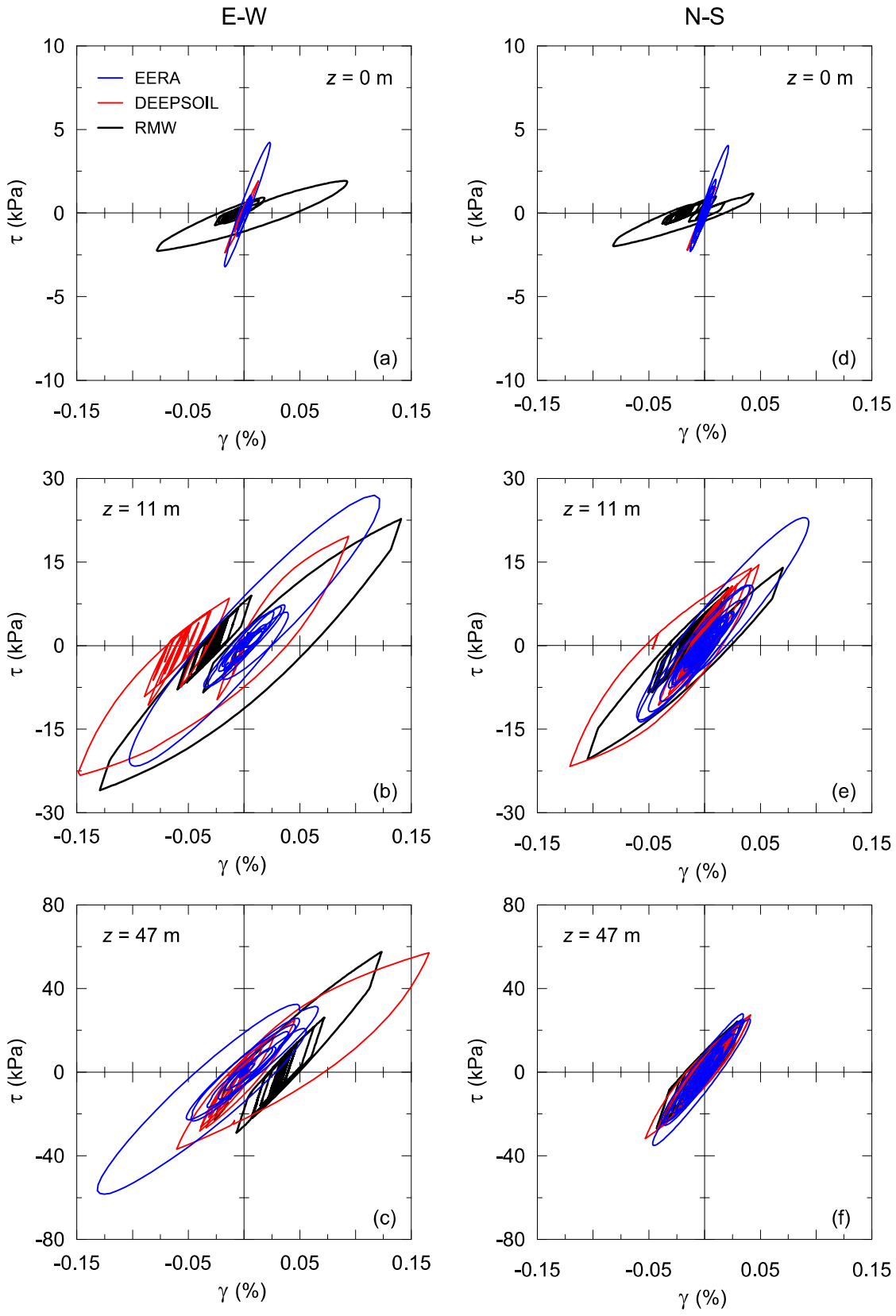

Fig. 11. Stress-strain curves predicted at different depths during the LSST07 event.

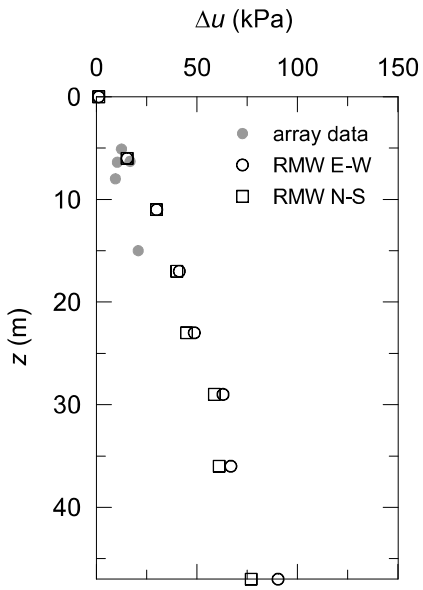

Fig. 12. Comparison between excess pore water pressure distributions predicted at the end of the SWANDYNE II analyses and the data recorded during the LSST16 event [55].

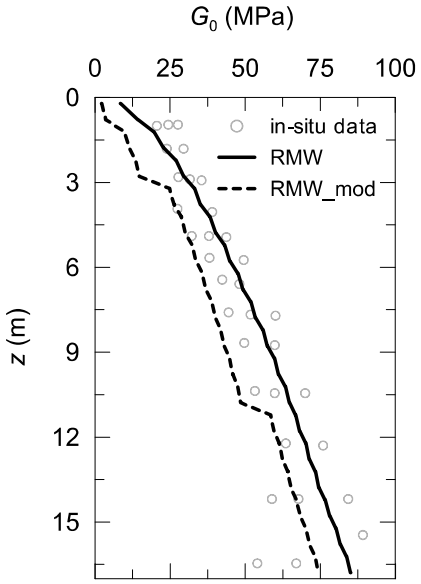

Fig. 13. Elastic shear modulus profiles adopted in the 17 m soil column analysis.

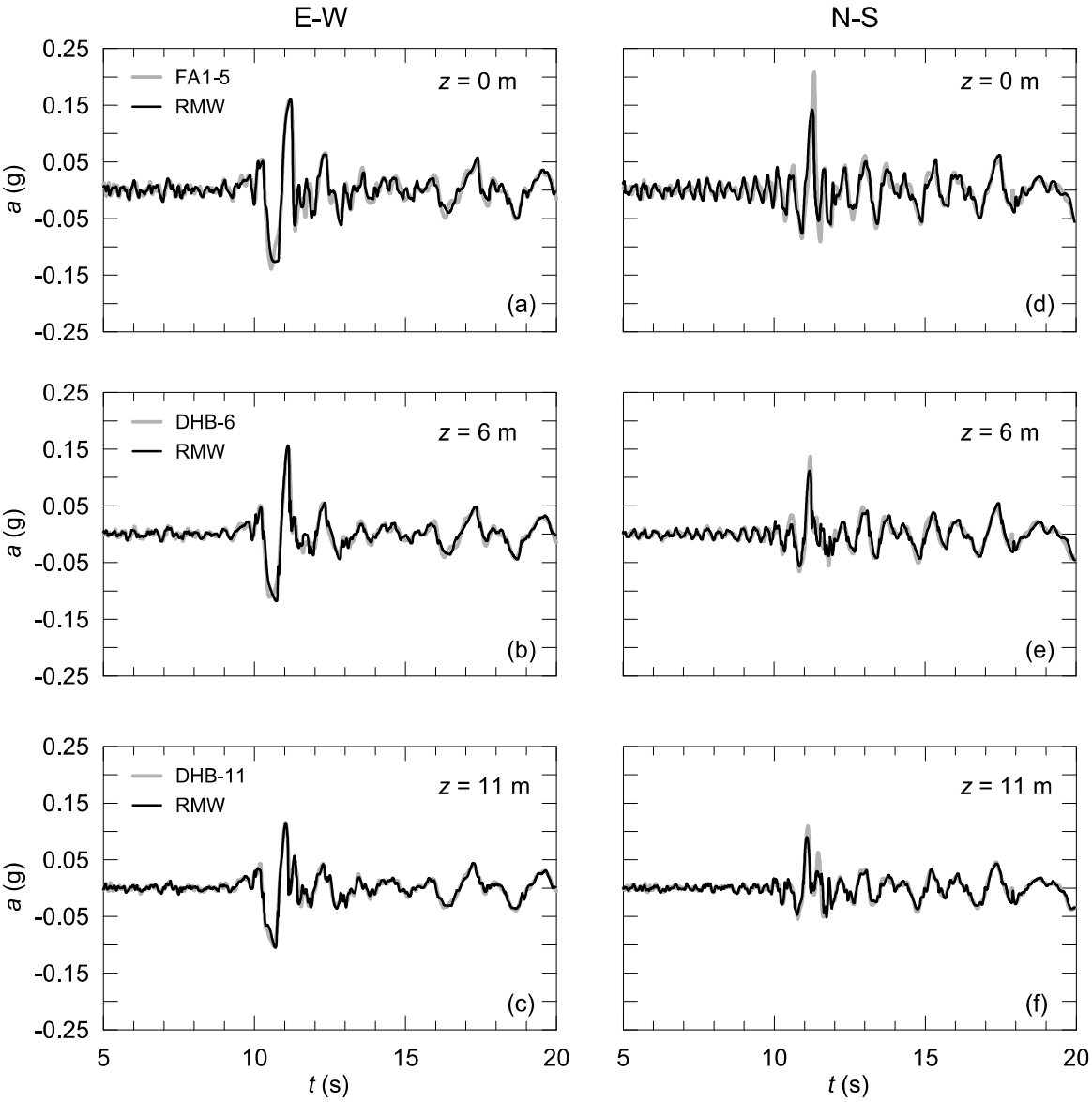

Fig. 14. Acceleration time histories obtained in the 17 m soil column analysis assuming the "RMW" profile.

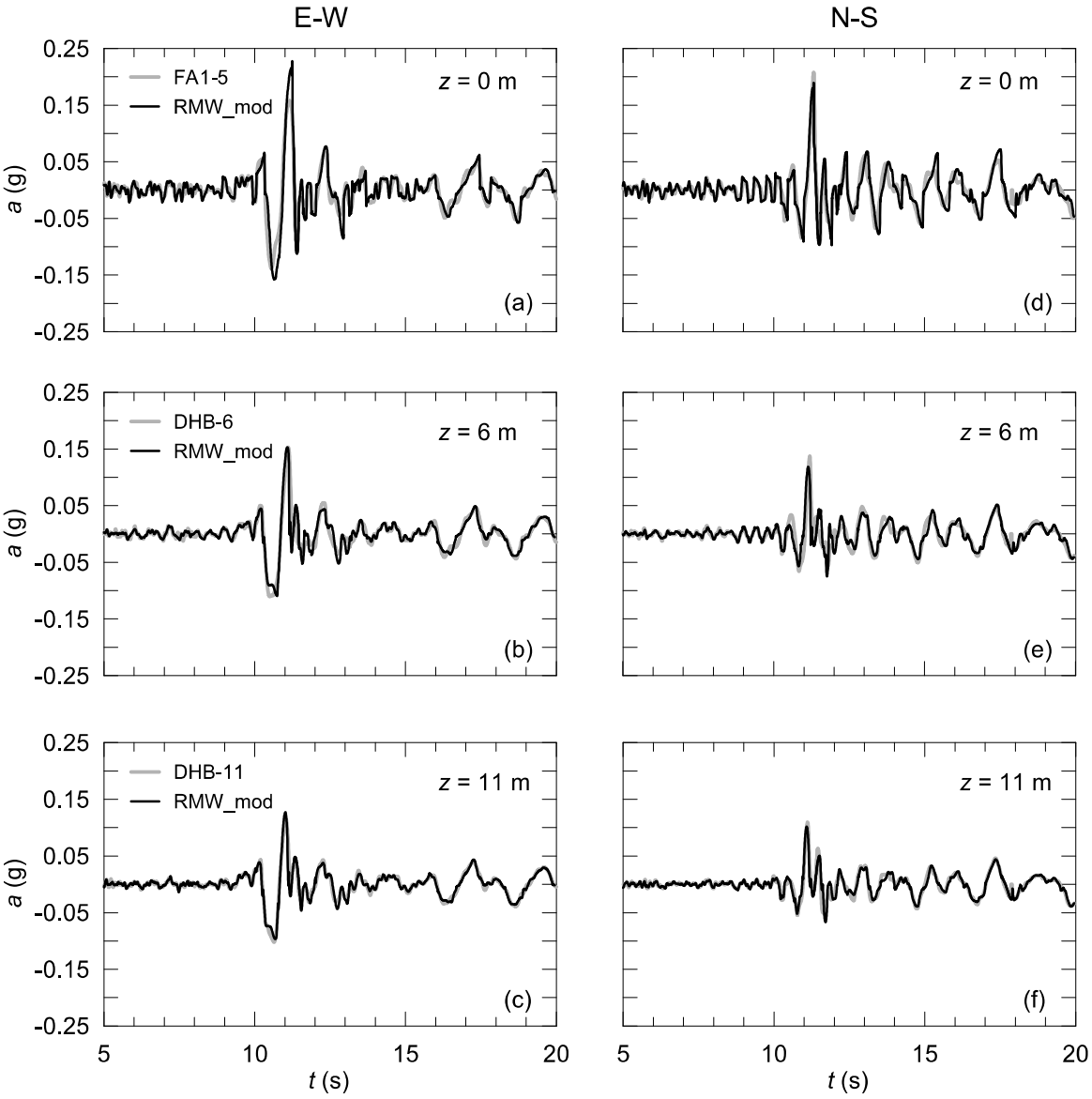

Fig. 15. Acceleration time histories obtained in the 17 m soil column analysis assuming the "RMW_mod" profile.

Table 1 Earthquakes recorded by the LSST array and used in the simulations

Date	Name	Focal depth (km)	Magnitude (M_L)	PGA (g)		
				E-W	N-S	V
17 July 1986	LSTT11	2.0	4.3	0.07	0.10	0.04
20 May 1986	LSTT07	15.8	6.2	0.16	0.20	0.04

Table 2 Material parameters for the MRDF pressure-dependent hyperbolic model

Depth	β	s	γ_r	ξ_{small} (%)	p_1	p_2	p_3
0-6 m	1.365	0.975	0.0536	1.0228	0.96	0.400	2.10
6-11 m	1.425	0.840	0.0516	1.2051	1.00	0.400	2.70
11-47 m	1.470	0.705	0.0536	1.3147	1.00	0.158	3.25

Table 3 Material parameters for the *RMW* model

Depth	λ^*	κ^*	M	R	B	ψ	r_0	A	m	n
0-17 m	0.03	0.0015	0.922	0.08	0.60	1.0	1.0	1500	0.36	0.82
17-23 m	0.03	0.0015	1.096	0.08	0.60	1.0	1.0	1900	0.36	0.82
23-29 m	0.03	0.0015	0.814	0.08	0.60	1.0	1.0	1350	0.36	0.82
29-36 m	0.03	0.0015	0.941	0.08	0.60	1.0	1.0	1900	0.36	0.82
36-47 m	0.03	0.0015	0.730	0.08	0.60	1.0	1.0	1150	0.36	0.82